Chemical Papers
https://doi.org/10.1007/s11696-025-04428-3

ORIGINAL PAPER

A serendipitous synthesis of N,N′-Diethyloxamide: crystallographic and computational analysis of its solid-state structure

Mahdi Jemai[1,2] · Miquel Barceló-Oliver[3] · Houda Marouani[1] · Antonio Frontera[3] · Rafel Prohens[1]

Received: 15 May 2025 / Accepted: 4 October 2025

Abstract

A combined crystallographic/computational analysis focused on the supramolecular features of the crystal structure of N,N′-diethyloxamide (NNDO) is discussed in this work. The studied compound was obtained unexpectedly during the synthesis of a series of salts of cyclic oximes derivatives. In the solid state NNDO is stabilized essentially through a strong N–H···O hydrogen bond but Hirshfeld surface analysis and Density Functional Theory (DFT) calculations were carried out to evaluate the strength of the predominant hydrogen bonds observed in the X-ray structure, as well as the secondary C–H···O and C–H···N contacts established between the ethyl groups and the perpendicular dioxamide group. These interactions were further investigated using a combination of Quantum Theory of Atoms in Molecules (QTAIM), Non-Covalent Interaction Plot (NCIplot) and natural bond orbital (NBO) analysis computational tools, and were rationalized using Molecular Electrostatic Potential (MEP) surface, electron localization function (ELF), localized orbital locator (LOL) and Fukui function calculations. The insights gathered in this study enrich the understanding of the factors governing crystal packing in amides and related compounds.

Keywords N,N′-Diethyloxamide · Crystal structure · Hirshfeld surface analysis · DFT calculations

Introduction

The success of chemical synthesis is closely tied to the anticipated reactivity of molecular functional groups (Kolb et al. 2001; Paul et al. 2018). However, alongside the expected outcomes, the discovery of unexpected new materials can also occur. Such compounds are valuable as they may provide insights into novel polymorphism or unique crystal structures, which could open new avenues for research (Heller et al. 2020; Carver et al. 2012).

In this study, N,N′-diethyloxamide (NNDO, see Scheme 1) was serendipitously obtained during an attempt to synthesize salts of Oxyma-T, a cyclic oxime derivative, as a part of another ongoing study. This amide has been successfully used in organic synthesis, particularly in the preparation of imidazole-based medicinal intermediates and various heterocyclic compounds (Abdullah et al. 2023; Chaudhury et al. 2015). In general oxalamides are currently used in materials science to design polymers (Casas et al. 2002) or in crystal engineering (Curtis et al. 2005) to mention only some of their multiple applications.

Moreover, although some works have described previously the prevalent hydrogen bonds across the N–H and C=O groups present in oxalamides (Hoffmann et al. 2005; Molina-Paredes et al. 2022; Dhanishta et al. 2018; Alemán et al. 2004; Coe et al. 1997; Podda et al. 2024) a deeper knowledge about solid-state secondary intermolecular interactions in members of this important family of compounds is much less studied, which motivated the analysis presented in this manuscript, which can enrich with new valuable structural data the understanding of the factors dictating crystal packing in amides and related

✉ Antonio Frontera
toni.frontera@uib.es

✉ Rafel Prohens
rafel_prohens@ub.edu

[1] Laboratory of Organic Chemistry, Faculty of Pharmacy and Food Sciences, Universitat de Barcelona, Av. Joan XXIII 27-31, 08028 Barcelona, Spain

[2] Laboratory of Material Chemistry, LR13ES08, Faculty of Sciences of Bizerte, University of Carthage, 7021 Bizerte, Tunisia

[3] Department of Chemistry, Universitat de Les Illes Balears, 07122 Palma, Spain

Published online: 17 October 2025

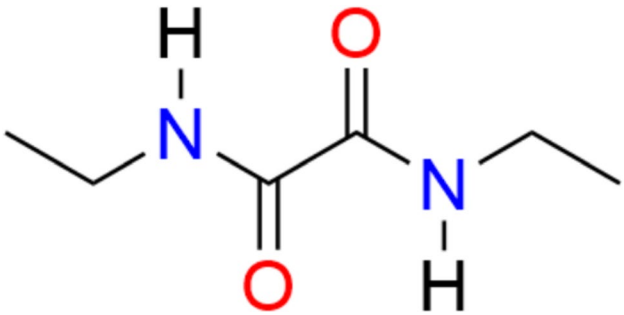

Scheme 1. Molecular structure of N,N'-diethyloxamide reported herein

compounds (Morales-Santana et al. 2022; Mahesha et al. 2025; Robello et al. 2021; Garg et al. 2025).

While the literature reports only the cell parameters for NNDO, we present here its single-crystal X-ray diffraction data and full 3D structure, thus allowing a detailed analysis and exploration of the interactions governing the crystal packing. To complement the experimental findings, Density Functional Theory (DFT) calculations were performed to assess the strength of the predominant hydrogen bonds observed in the X-ray structure, as well as the C–H···O and C–H···N contacts formed between the ethyl groups and the perpendicular NC(O)C(O)N system (oxamide group). These interactions were further analyzed using a combination of Quantum Theory of Atoms in Molecules (QTAIM), Non-Covalent Interaction Plot (NCIplot) and natural bond orbital (NBO) analysis computational methods, providing detailed in-sights into their nature. Additionally, Molecular Electrostatic Potential (MEP) surface, localized orbital locator (LOL) and Fukui function calculations were employed to rationalize these interactions, offering a comprehensive understanding of the molecular and supramolecular features of the compound.

Materials and methods

Synthesis and crystallization

The single crystal of the title compound was unexpectedly obtained in a two-step's synthesis of Oxyma-T salt with DABCO. In the first step Oxyma-T was synthesized following a procedure reported in the literature by Fernando Albericio and co-workers (Jad et al. 2016) as follows: the stirring between 1,3-diethyl-2-thiobarbituric acid, sodium hydroxide, sodium nitrite, acetic acid and hydrochloric acid in the presence of methanol and water as solvent followed by slow evaporation of the synthesized material produced Oxyma-T as expected in yield 96%. However, in the second step, when trying to grow single crystals of the salt formed between Oxyma-T and 1,4-Diazabicyclo[2.2.2]octane (DABCO) in ethanol at 40 °C, instead of the expected salt needles of NNDO suitable for single crystal X-ray diffraction (SCXRD) analysis were isolated and analyzed. Interestingly, when trying to recrystallize Oxyma-T in water/methanol at 70 °C in the absence of DABCO crystals suitable for SCXRD were isolated and again the expected Oxyma-T was not crystallized. Instead, 1,3-diethylimi-dazole-2-thione-3,4-dione (DDTD) was identified through SCXRD (data not shown), a compound previously reported by Kelley et al. (Kelley et al. 2020). It is known that oximes when heated in the presence of strong acids or bases undergo a process known as Beckman rearrangement (Heldt et al. 1958; Orlandin et al. 2022), which explains the formation of both compounds according to the proposed mechanisms depicted in Schemes 2 and 3.

Powder X-ray diffraction (PXRD) patterns were recorded on a Bruker D2 Phaser diffractometer in Bragg–Brentano reflection geometry using a Cu Kα radiation source ($\lambda = 1.5406$ Å) and a Si–Einkristall monochromator. Figure 1 presents the experimental PXRD patterns of NNDO (a) and Oxyma-T (b), alongside their simulated patterns derived from single-crystal data (c and d, respectively). The good

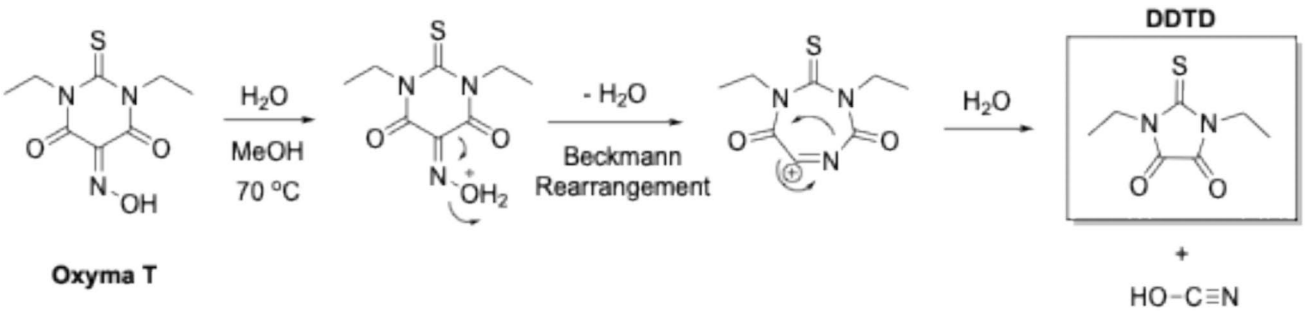

Scheme 2. Suggested synthetic mechanism in the formation of DDTD

Scheme 3. Suggested synthetic mechanism in the formation of NNDO

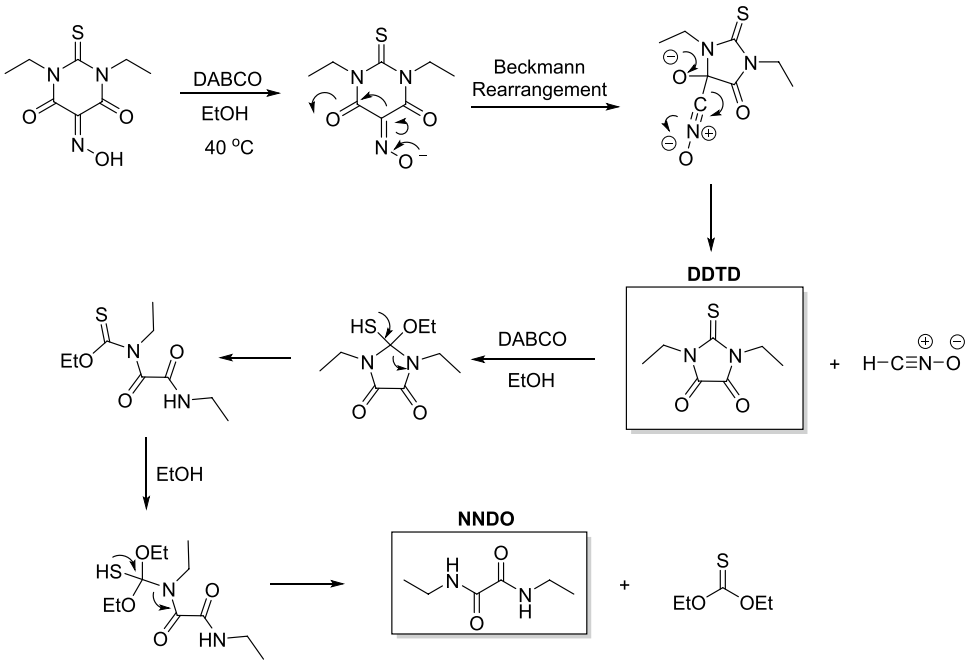

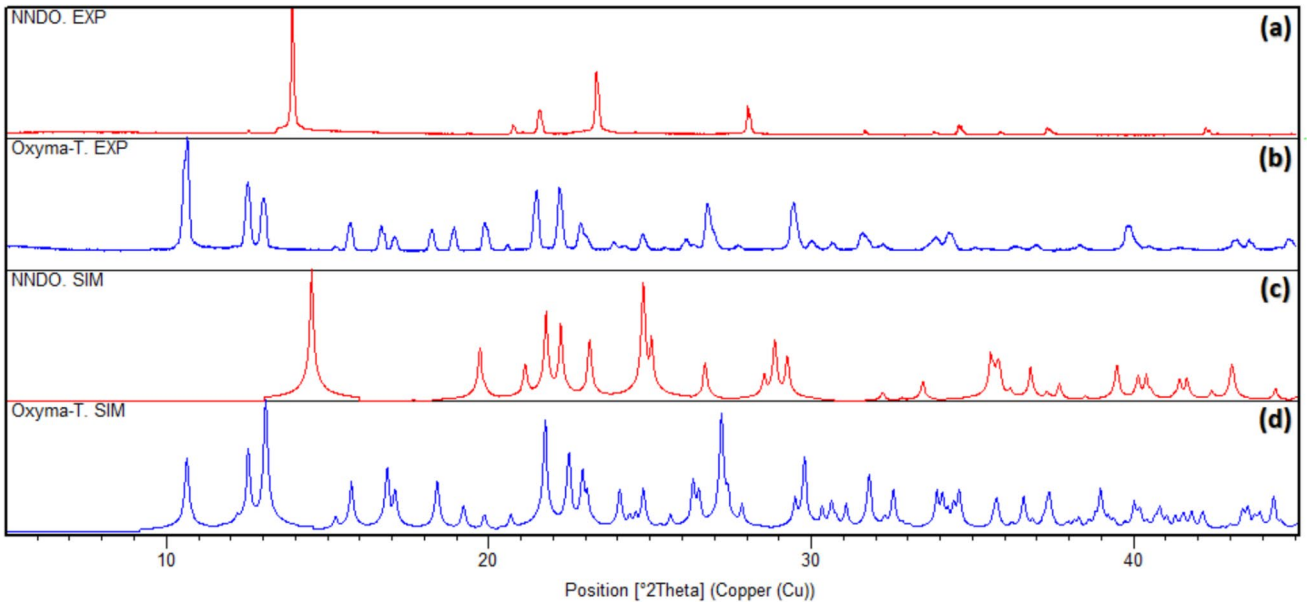

Fig. 1 **a**, **b** Experimental (EXP) Powder X-ray diffraction patterns of NNDO and Oxyma-T, respectively; **c**, **d** simulated (SIM) patterns

agreement between experimental and simulated patterns confirms the phase purity of both compounds.

Crystallography data

The crystallographic data for NNDO in this study were obtained using a D8 VEN-TURE Bruker AXS diffractometer, equipped with an Incoatec high brilliance IμS DIAMOND Cu tube (Cu Kα radiation, $\lambda = 1.54178$ Å) and an Incoatec Helios MX multilayer optics. Data reduction and cell refinements were performed using the Bruker APEX5 pro-gram (Bruker 2023). The multi-scan method was then employed to correct the data collected using the SAD-ABS-2016/2 program (Bruker 2023). Under *Olex2-1.5* suite (Dolomanov et al. 2009), crystal structure was solved via intrinsic phasing with SHELXT-2018/2 and refined via full matrix least squares technique with *SHELXL-2019/3* (Sheldrick et al. 2015). Refinement of all the non-hydrogen

atoms were carried out with anisotropic thermal parameters by full-matrix least squares calculations on F^2. A difference map was used to localize and refine nitrogen-bonded hydrogen atoms. Hydro-gen atoms bonded to carbon were then introduced at calculated positions and refined as riding atoms, with $U_{iso}(H) = 1.2U_{eq}(C)$. The structure was checked for higher symmetry with the help of the program *PLATON* (Spek et al. 2003). Crystal data, data collection and structure refinement details are summarized in Table 1.

The Cambridge structural database reveals that only the cell parameters related to NNDO structure are available (CSD ref-codes: GAHXIX, CCDC:1,163,044) but not its 3D structure. The previously available data has the following cell parameters: Space Group: $P2_1/n$, $a = 5.077$ (1) (5) Å, $b = 10.016$ (1) Å, $c = 8.226$ (1) Å and $\beta = 97.80$ (1) (14)° while the structure reported herein have the following cell parameter: Space Group: $P2_1/n$ $a = 5.0669$ (5) Å, $b = 10.0285$ (10) Å, $c = 7.7373$ (8) Å, $\beta = 96.915$ (5) (Desseyn et al. 2004). Table 1 shows the complete crystallographic parameters.

Theoretical methods

For the DFT calculations of the supramolecular assemblies, the PBE0-D3/def2-TZVP level of theory was employed using the Gaussian 16 software package (Frisch et al. 2016; Adamo et al. 1999; Grimme et al. 2010; Weigend. 2006). The binding energies were determined as the difference between the total energy of the assembly and the sum of the energies of the isolated monomers, with corrections applied for the basis set superposition error (BSSE) (Boys and Bernardi 1970). The molecular electrostatic potential (MEP) surfaces were calculated using the 0.001 a.u. isosurface to approximate the van der Waals envelope.

To analyze the interactions within the assemblies, QTAIM (Bader 1998) and NCIPlot methods were applied at the same level of theory using the AIMAll software (Keith 2013). The NCIPlot method (Contreras-García et al. 2011; Johnson et al. 2010) is particularly effective for visualizing noncovalent interactions in real space. It employs reduced density gradient (RDG) isosurfaces and a color-coded scheme based on the sign of the second eigenvalue of the electron density Hessian (λ_2) to differen-tiate between attractive and repulsive interactions. For this study, the settings used were RDG = 0.5, density cut-off = 0.04 a.u., and a color scale ranging from –0.04 a.u. $\leq \text{sign}\lambda_2(\rho) \leq$ 0.04 a.u. Strongly attractive interactions are represented in blue, while moderately attractive interactions are shown in green.

Electron localization function (ELF) (Becke et al. 1990), localized orbital locator (LOL) (Becke et al. 1990) and Fukui functions (Fukui et al. 1952) were computed at the same level using Multiwfn program (Lu et al. 2012). The natural bond orbital (NBO) analysis was performed using NBO 7.0 program (**NBO 7.0:** Glendening et al. 2018).

Table 1 Crystal data of NNDO

Chemical formula	$C_6H_{12}N_2O_2$
M_r	144.18
Formula weight (g mol^{-1})	144.18
Crystal system, space group	Monoclinic, $P2_1/n$
Temperature (K)	100
a, b, c (Å)	5.0669 (5), 10.0285 (10), 7.7373 (8)
B (°)	96.915 (5)
V (Å)	390.30 (7)
Z	2
Radiation type	Cu $K\alpha$
μ (mm^{-1})	1.54178
Crystal size (mm)	0.34 × 0.11 × 0.06
Absorption correction (Multi-scan): T_{min}, T_{max}	0.480, 0.753
Reflections collected	4207
Independent reflections	705
Reflections with $I > 2\sigma(I)$	660
R_{int}	0.0489
Refined parameters	51
R[$F^2 > 2\sigma(F^2)$]	0.0477
$wR(F^2)$	0.1334
Goodness-of-fit on F^2	1.071
CCDC	2,420,343

Results and discussion

Structural description

NNDO is a diamide with the chemical formula $C_6H_{12}N_2O_2$. It crystallizes in the monoclinic system with the space group $P2_1/n$ and half molecule in the asymmetric unit. NNDO is a centrosymmetric molecule with an inversion center located at the midpoint of the C_2–C_2 bond. The molecular motifs are distributed within the monoclinic system at the vertices and

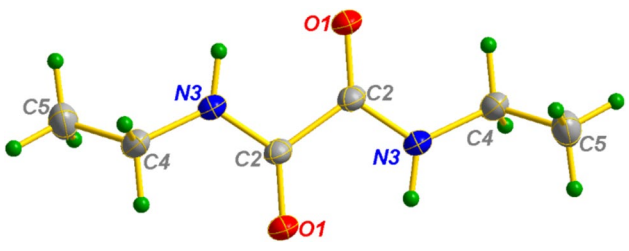

Fig. 2 Ortep representation of the structure of NNDO with the labeling scheme. Ellipsoids are drawn at 35% probability level

the center of the unit cell (Fig. 2). To better describe the arrangement of NNDO within the crystal lattice, the structure was projected onto the $\left(\vec{b},\vec{c}\right)$ plane, which offers the clearest view of the atomic arrangement, as shown in Fig. 3. This projection reveals that NNDO molecules are packed in a "zig-zag" pattern along both the $y=0$ and $y=1/2$ axes within the crystal cell.

Supramolecular features

In the NNDO structure, the interactions which play a crucial role in structural cohesion and molecular packing are the N–H···O hydrogen bonds, for which the geometrical parameters are detailed in Table 2 and illustrated in Fig. 4(b). Moreover, the attachment between NNDO molecules via auxiliary C–H···O and C–H···N interactions leads to the formation of an $R_2^2(8)$ supramolecular unit allowing the interconnection between the NNDO "zig-zag" layers mentioned in Sect. "Structural description" (Bernstein 1991).

The projection of the NNDO structure along the $(\vec{a},\vec{c})$ plane as shown in Fig. 4a show that N–H···O are interlinking between molecules in layers parallel to the $(\vec{a},b)$ plane, positioned at $z=0$ and $z=1/2$. Upon bonding, the NNDO molecules form an $R_2^2(10)$ interaction motif, as shown in Fig. 4b, which further enhances the hydrogen-bonding network within these layers, contributing to the stability and integrity of the crystal structure.

Hirshfeld surface analysis

To get a deeper insight into the supramolecular features of the NNDO structure, Hirshfeld surface analysis has been conducted. Figure 5 illustrates an overview of the distribution of the different non-covalent interactions present in the NNDO structure (Spackman and Jayatilaka 2009; Spackman and McKinnon 2002; Mackenzie et al. 2017). Crystalexplorer 3.1 software version was used in this study, the normalized contact distance (d_{norm}) and the shape index mode

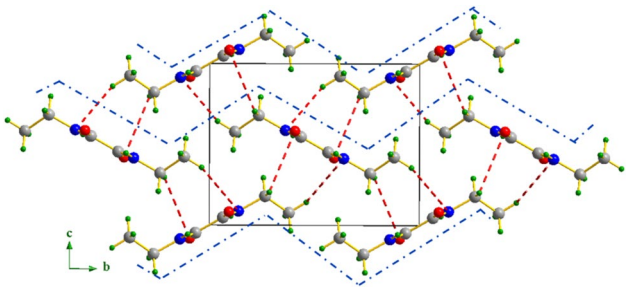

Fig. 3 Projection of the NNDO structure along the $(\vec{b},\vec{c})$ plane, The blue dashed lines highlight the alternating orientation of NNDO molecules along the y-axis

Table 2 Hydrogen-bond geometry in NNDO (Å, °)

D–H…A	D–H (Å)	H…A (Å)	D…A (Å)	D–H…A (°)
N3–H3···O1^{ii}	0.91 (2)	2.05 (2)	2.8752 (17)	151 (2)
N3–H3···O1^{i}	0.91 (2)	2.27 (2)	2.7086 (17)	109 (1)
C4–H4A···O1^{iii}	0.99	2.72	3.513 (2)	138
C5–H5C···N3^{iv}	0.98	2.85	3.734 (2)	151

Symmetry codes: (i) $-x+1,-y+1,-z+1$; (ii) $x-1$, y, z; (iii) $x-1/2,-y+1/2,z+1/2$; (iv) $-x+1/2,y-1/2,-z+3/2$

were performed using rescaled surface property ranges of −0.5–1.5 and from −1–1 Å respectively. The corresponding 2D fingerprint plots were generated with both internal (d_i) and external (d_e) distances over the range [0.4 Å–2.6 Å].

Figure 5a draw up the d_{norm} surface, which is a 3D visual mapping showing the full ex-tent of non-covalent interactions that can be observed in the crystal displayed in red,

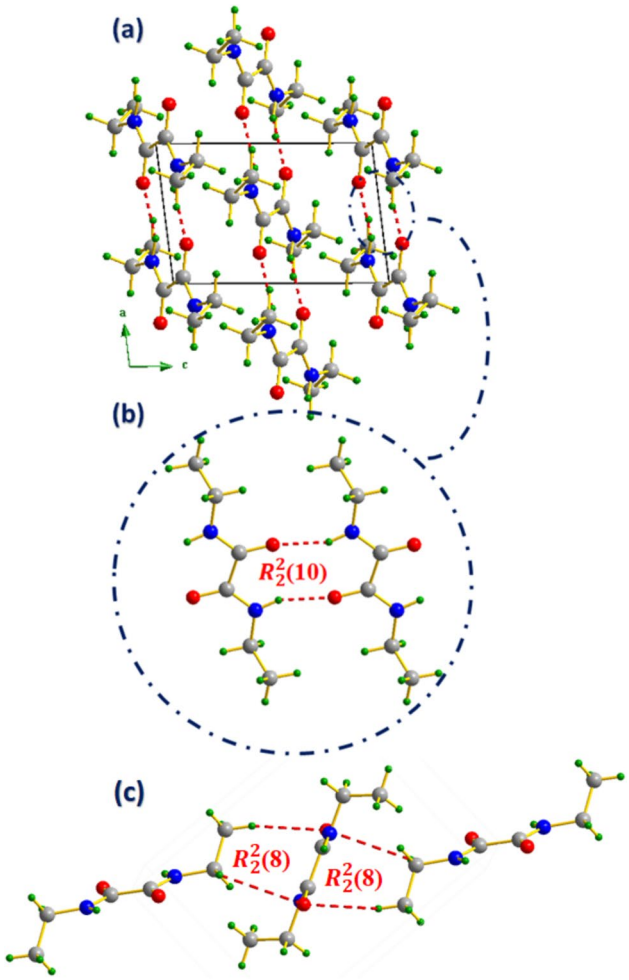

Fig. 4 **a** Projection of the NNDO structure along the $(\vec{a},\vec{c})$ plane **b** amide/amide intermolecular $R_2^2(10)$ interaction motif, **c** auxiliary C–H···O and C–H···N intermolecular $R_2^2(8)$ interaction motif. Relevant intermolecular contacts are represented by a dashed red line

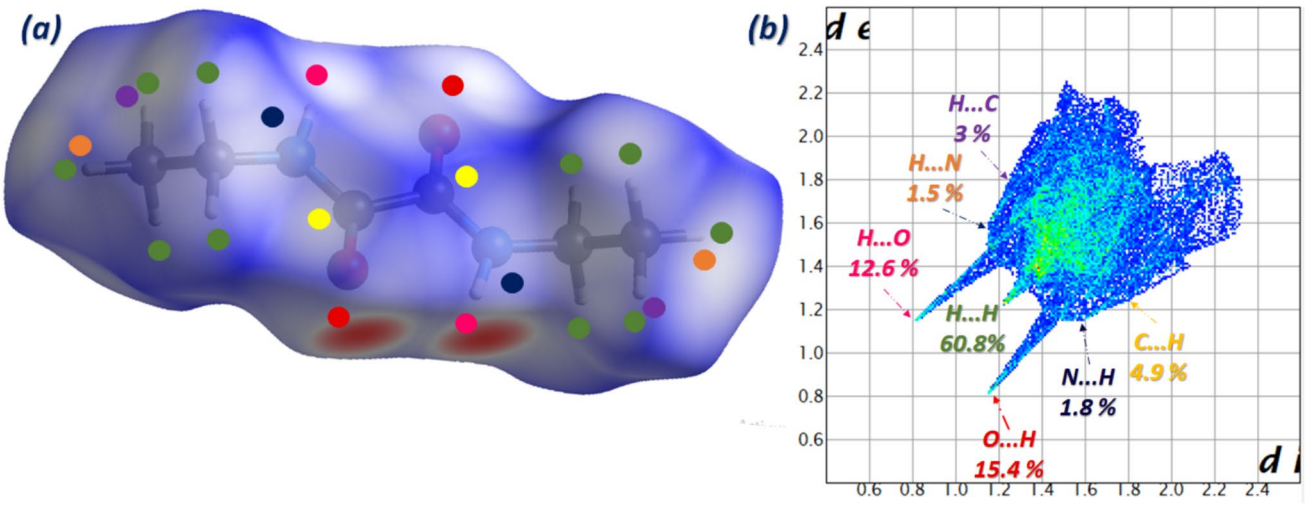

Fig. 5 Hirshfeld surface mapped over d_{norm} mode for NNDO **a** and its two-dimensional fingerprint plots **b**

white and blue colors; respectively for interatomic contacts shorter than the sum of the van der Waals radius (usually but not limited to H-bonds), equal to the sum of van der Waals radius (usually corresponding to weak van der Waals interactions) as well as those longer than the sum of van der Waals radius (corresponding to long and non-bonding contacts). The 2D fingerprints plot illustrated in Fig. 5 (b) supply a quantitative description on the relative contribution of each interaction in the molecule. The highest percentage of inter-molecular close-contacts corresponds to the H···H contact (which can be considered as repulsive or steric interactions) with 60.8%, while the next percentage goes to the H–bonding N–H···O and C–H···O (O···H/H···O contacts) with a percentage equal to 28%, which is the principal contact contributing to intermolecular attachment. The remaining percentage, 10.9%, is divided between the remaining contacts, which are H···C/C···H (7.9%) and H···N/N···H (3.3%), with a residual contribution to the stabilization of the crystal. The Enrichment ratios (ER) were calculated according to the method proposed by Jelsch et al. (Jelsch et al. 2014), based on Hirshfeld surface data. The atomic surface contributions were *H* (80.4%), *O* (14.0%), *C* (3.95%), and *N* (1.65%). The observed ER values are: $ER_{HH} = 0.94$, $E_{HO} = 1.24$, $ER_{HC} = 1.24$, and $E_{HN} = 1.24$. These values reflect a preferential formation of H···O, H···C, and H···N contacts in the crystal.

DFT calculations

To investigate the electron deficient and electron rich regions of the NNDO molecule, we computed MEP, ELF, LOL and Fukui function. The MEP surface, shown in Fig. 6, reveals that the minimum is located at the oxygen atoms (−36.7 kcal/mol), while the maximum is at the N–H groups (30.7 kcal/mol), as anticipated. These significant MEP values suggest the potential for strong hydrogen bonds, including the formation of the $R_2^2(10)$ interaction motif discussed in Sect. "Hirshfeld surface analysis", which propagates the molecules into a 1D polymeric structure. Additionally, positive MEP values were observed at the hydrogen atoms of the methyl groups (13.8 kcal/mol) and at the center of the C(O)–C(O) bond, perpendicular to the oxamide group plane (7.8 kcal/mol), highlighting other regions of potential interaction.

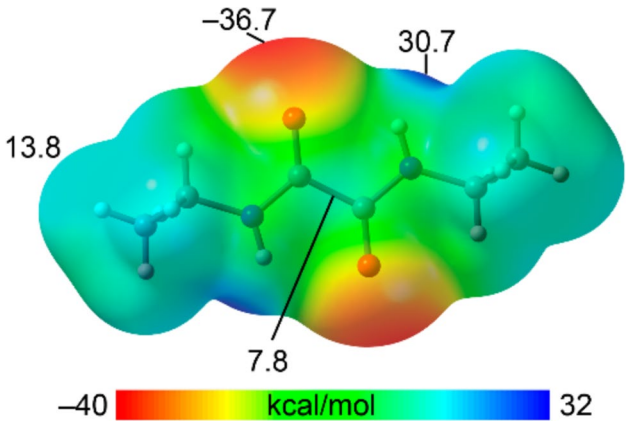

Fig. 6 MEP surface of NNDO molecule. MEP values at selected points of the surface are given in kcal/mol. Isovalue 0.001 a.u

Figure 7 presents the 2D-ELF, 2D-LOL, and Fukui function analyses of N,N′-diethyloxamide. The 2D-ELF analysis (a) clearly shows electron localization, particularly identifying lone pairs at the oxygen atoms. It also depicts the typical concentration of electrons associated with covalently bonded hydrogen atoms. A distinction can also be observed between the C=C double bond and the N–C single bonds.

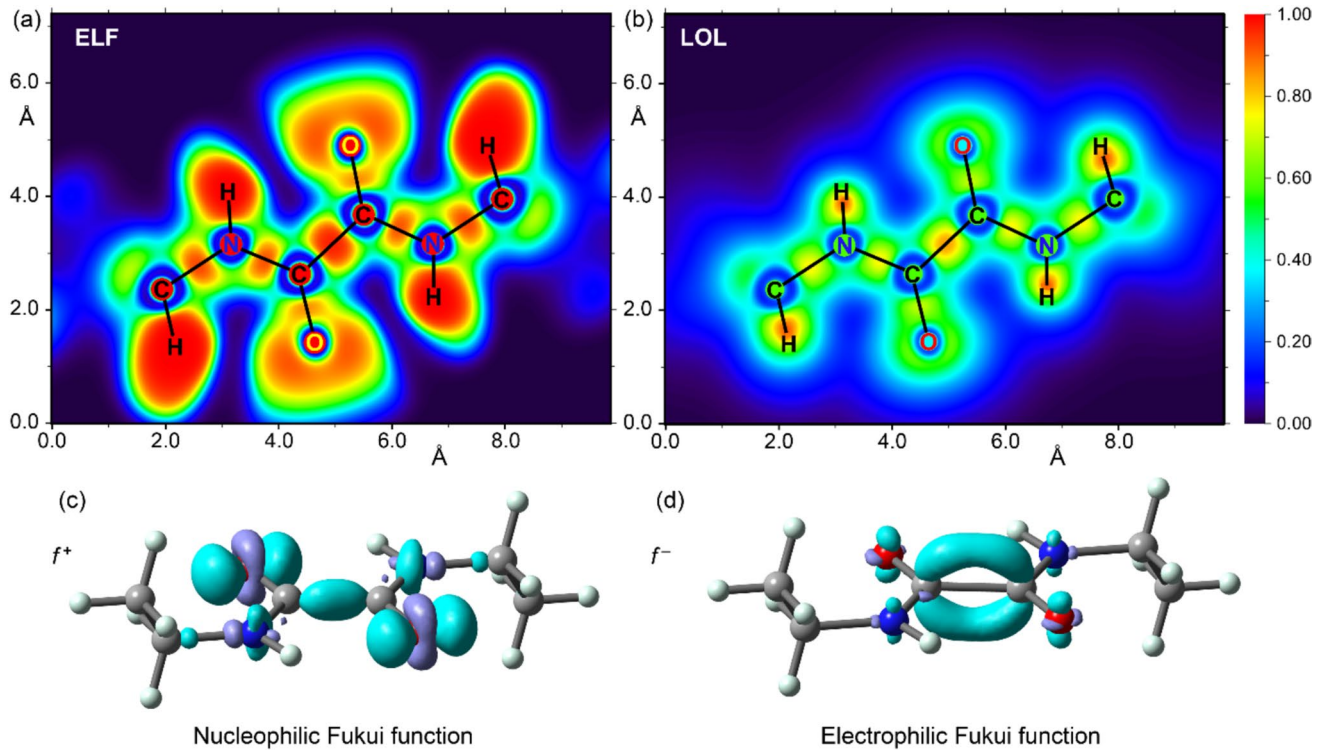

Fig. 7 Topological and reactivity analyses of N,N'-diethyloxamide (NNDO). **a** 2D-ELF and **b** 2D-LOL plots showing electron localization. **c** Isosurface of the nucleophilic Fukui function (f^+) at 0.01 a.u., highlighting the most reactive sites for electrophilic attack. **d** Isosurface of the electrophilic Fukui function (f^-) at 0.01 a.u., indicating the most reactive sites for nucleophilic attack

The 2D-LOL analysis (b) yields similar results, showing localized electrons at the C=C bonds and on the hydrogen atoms.

Regarding the nucleophilic and electrophilic behavior of NNDO, this can be deduced from the Fukui functions, f^+ and f^-, respectively. The nucleophilic Fukui function (f^+ in Fig. 7c) shows that the regions most likely to act as a nucleophile (react with an electrophile) are primarily located at the carbonyl carbon atoms, as indicated by the isosurfaces. Conversely, the electrophilic Fukui function (f^- in Fig. 7d) shows that the regions most likely to act as an electrophile (reacting with a nucleophile) are located at the central C=C bond, as indicated by the isosurfaces.

Next, we analyzed two different assemblies extracted from the X-ray structure of NNDO to study and compare the energetic characteristics of the noncovalent interactions described in Sect. "Supramolecular features". The analysis employed the QTAIM and NCIplot methods, which, when combined in the same representation, provide valuable insights into noncovalent interactions in real space. Two trimers were selected for this study (Fig. 8): one featuring the dominant N–H···O hydrogen bonds (Fig. 7a) and another where a central NNDO molecule interacts with the ethyl groups of two adjacent molecules above and below the oxamide group plane through C–H···N and C–H···O contacts

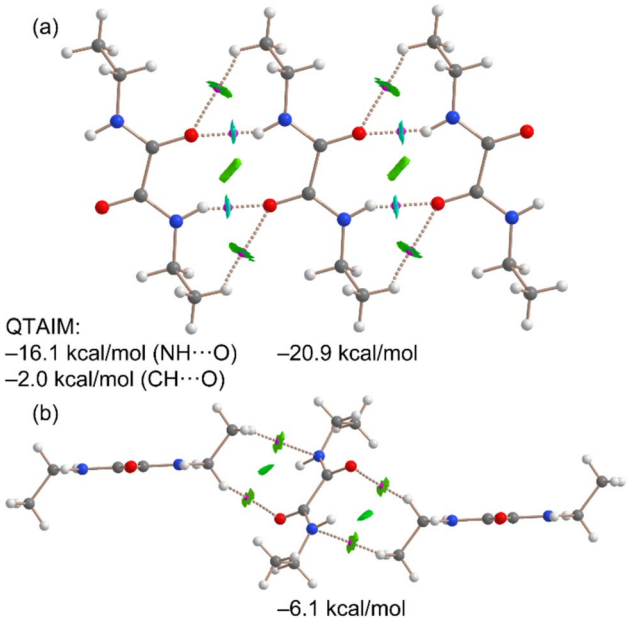

Fig. 8 QTAIM (BCPs in fuchsia and bond path as dashed bonds) and NCIplot (RDG = 0.5, ρ cut-off = 0.04 a.u., color scale –0.035 a.u. $\leq (\text{sign}\lambda 2)\rho \leq 0.035$ a.u. for the H-bonded **a** and C–H···N,O bonded **b** trimers. The energies of the assemblies and those derived from potential energy densities are indicated

(Fig. 8b). This latter assembly is particularly relevant for understanding the overall 3D architecture of the compound, as it connects the hydrogen-bonded 1D polymers to form the extended crystal structure.

The QTAIM analysis of the H-bonded trimer reveals that each N–H···O interaction is characterized by a bond critical point (BCP, represented as pink spheres) and a bond path (dashed lines) connecting the oxygen and hydrogen atoms. These hydrogen bonds are further highlighted by blue reduced density gradient (RDG) isosurfaces that coincide with the locations of the BCPs. Notably, the combined QTAIM/NCIPlot analysis also identifies ancillary C–H···O interactions involving the C–H bonds of the ethyl groups, confirmed by the presence of BCPs, bond paths, and green RDG isosurfaces linking the hydrogen and oxygen atoms. The interaction energy of the trimeric assembly is calculated to be –20.9 kcal/mol, underscoring the strong nature of the N–H···O hydrogen bonds and their significance in the solid-state structure of NNDO.

To evaluate the relative contributions of the C,N–H···O interactions, the strength of the hydrogen bonds was analyzed using QTAIM parameters, specifically the potential energy density values measured at the BCPs characterizing the hydrogen bonds. The results indicate that the N–H···O hydrogen bonds contribute −16.1 kcal/mol, while the C–H···O inter-actions account for −2.0 kcal/mol, confirming the predominant role of the N–H···O interactions. These findings are consistent with the molecular electrostatic potential (MEP) sur-face analysis. The total interaction energy, estimated using the QTAIM energy predictor ($E = ½$ x V), is −18.1 kcal/mol, which closely matches the −20.9 kcal/mol obtained from the supramolecular approach. This agreement underscores the reliability of the QTAIM methodology for analyzing hydrogen bond interactions.

The QTAIM analysis of the trimer, where two NNDO molecules are positioned above and below the plane defined by the oxamide group of the central molecule, is shown in Fig. 8b. This analysis reveals that two hydrogen atoms of the ethyl groups form interactions with the oxygen and nitrogen atoms of the oxamide group, characterized by two bond critical points (BCPs) and bond paths. Additionally, these interactions are visualized as green RDG isosurfaces located between the oxamide and ethyl groups. The binding energy of this trimer is weaker compared to the hydrogen-bonded trimer (−6.1 kcal/mol), as anticipated, confirming the dominance of N–H···O interactions. Nevertheless, the C–H···O,N interactions also play a significant role in dictating the crystal packing of NNDO.

Natural Bond Orbital (NBO) analysis was used to characterize the orbital interactions within the trimer, as shown in Fig. 9. This analysis reveals a significant charge transfer from the lone pair of the oxygen atom, LP(O), to the antibonding $\sigma*$(N–H) orbital. The second-order stabilization

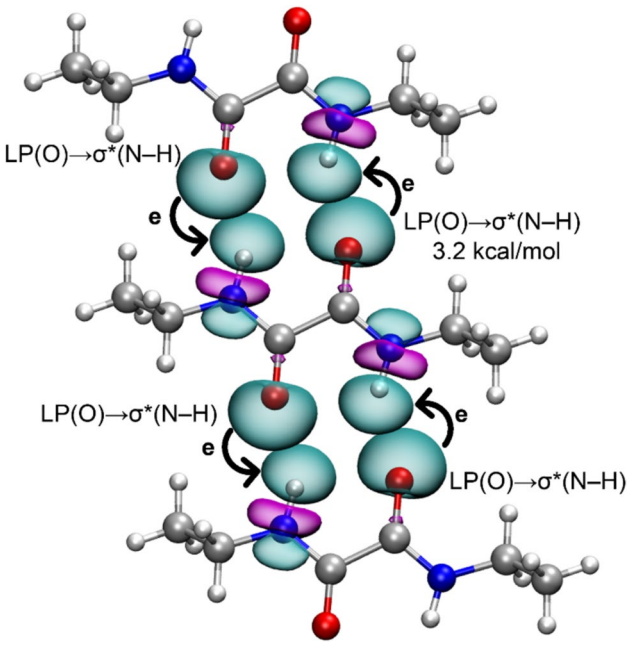

Fig. 9 Natural Bond Orbital (NBO) analysis of the trimer of N,N'-diethyloxamide, showing the LP(O)→$\sigma*$(N–H) orbital interactions. The electron transfer from the oxygen lone pair (LP(O)) to the antibonding N–H orbital ($\sigma*$(N–H)) is represented by the arrows

energy for this donor–acceptor interaction is 3.2 kcal/mol for each N–H···O hydrogen bond. Since there are four such interactions within the trimer, the total orbital stabilization energy is 12.8 kcal/mol. This result confirms the importance of orbital donor–acceptor charge transfer in this system, which is consistent with the short N–H···O distances that facilitate optimal orbital overlap.

Conclusions

In summary, the crystal structure and noncovalent interaction analysis of N,N'-diethyloxamide (NNDO) reveal a well-organized supramolecular architecture dominated by N–H···O hydrogen bonds, which form the primary framework of the 1D polymeric arrangement. Hirshfeld surface analysis highlights the contribution of additional interactions, such as C–H···O and C–H···N contacts, to the crystal packing. Complementary DFT calculations further support the strength and significance of these interactions, with QTAIM, NBO and NCIplot analyses providing a detailed visualization of their role in the supramolecular structure. The insights gained from this study, including the comprehensive characterization of hydrogen bonds and secondary contacts, enhance our understanding of the factors governing crystal packing in amides and related compounds, offering valuable information for future explorations in crystal engineering and supramolecular chemistry.

Supplementary Information The online version contains supplementary material available at https://doi.org/10.1007/s11696-025-04428-3.

Acknowledgements The authors would like to acknowledge the CTI (UIB) for computational facilities. We also thank Prof. Fernando Albericio (University of KwaZulu-Natal, South Africa & University of Barcelona, Spain), Prof. Ayman El-Faham (Alexandria University, Egypt & Dar Al Uloom University, Saudi Arabia) and Prof. Mercedes Amat (University of Barcelona) for stimulating discussions regarding the synthetic mechanisms described in our work. This article is dedicated to Prof. Dr. Mercedes Amat on the occasion of her retirement.

Author contributions Conceptualization, A.F. and R.P.; methodology, M.J, R.P., H. M., M.B-O. and A.F.; validation, R.P., A.F.; formal analysis, M.J., R.P. and A.F.; investigation, A.F., R.P. and M.J.; resources, R.P. and A.F.; data curation, M.J.; writing—original draft preparation, M.J., A.F. and R.P.; writing—review and editing, M.J, R.P., H. M., M.B-O. and A.F.; supervision: R.P.; project administration, A.F. and R.P.; funding acquisition, A.F. and R.P. All authors have read and agreed to the published version of the manuscript.

Funding Open Access funding provided thanks to the CRUE-CSIC agreement with Springer Nature. This research was supported by the Research Project of MICIU/AEI of Spain (projects PID2020-115637GB-I00, PID2023-148453NB-I00 and PID2023-146632OB-I00 FEDER funds).

Data availability Crystallographic data have been deposited at the CCDC under CCDC number 2420343 and can be obtained from https://www.ccdc.cam.ac.uk.

Declarations

Conflict of interests The authors declare no conflict of interest.

References

Abdullah S, Ganguly S (2023) An overview of imidazole and its analogues as potent anticancer agents. Future Med Chem 15:1621-1646.

Adamo C, Barone V (1999) Toward reliable density functional methods without adjustable parameters: the PBE0 model. J Chem Phys 110:6158-6170.

Alemán C, Casanovas J (2004) Analysis of the oxalamide functionality as hydrogen bonding former: geometry, energetics, cooperative effects, NMR chemical characterization and implications in molecular engineering. J Mol Struct THEOCHEM 675:9-17.

Bader RFW (1998) A bond path: a universal indicator of bonded interactions. J Phys Chem A 102:7314-7323.

Becke AD, Edgecombe KE (1990) A covalent electron localization function. J Chem Phys 92:5397-5403.

Bernstein J (1991) Polymorphism of l-glutamic acid: decoding the α-β phase relationship via graph-set analysis. Acta Crystallogr B 74:1004-1010.

Boys SF, Bernardi F (1970) The calculation of small molecular interactions by the differences of separate total energies. Some procedures with reduced errors. Mol Phys 19:553-566.

Bruker (2023) Bruker AXS Inc., Madison, Wisconsin, USA.

Carver KM, Snyder RC (2012) Unexpected polymorphism and unique particle morphologies from monodisperse droplet evaporation. Ind Eng Chem Res 51:15720-15728.

Casas MT, Armelin E, Alemán C, Puiggalí J (2002) On the crystalline structure of even polyoxalamides. Macromolecules 35:8781-8787.

Chaudhury D, Banerjee J, Sharma N, Shrestha N (2015) Routes of synthesis and biological significances of Imidazole derivatives: review. World J Pharm Pharm Sci 3(8):1471-1746.

Coe S, Kane JJ, Nguyen TL, Toledo LM, Wininger E, Fowler FW, Lauher JW (1997) Molecular symmetry and the design of molecular solids: the oxalamide functionality as a persistent hydrogen bonding unit. J Am Chem Soc 119:86-93.

Contreras-García J, Johnson ER, Keinan S, Chaudret R, Piquemal JP, Beratan DN, Yang W (2011) NCIPLOT: a program for plotting noncovalent interaction regions. J Chem Theory Comput 7:625-632.

Curtis SM, Le N, Fowler FW, Lauher JW (2005) A rational approach to the preparation of polydipyridyldiacetylenes: an exercise in crystal design. Cryst Growth des 5:2313-2321.

Desseyn HO, Perlepes SP, Clou K, Blaton N, Van der Veken BJ, Dommisse R, Hansen PE (2004) Theoretical, structural, vibrational, NMR, and thermal evidence of the inter- versus intramolecular hydrogen bonding in oxamides and thiooxamides. J Phys Chem A 108:5175-5182.

Dhanishta P, Mishra SK, Suryaprakash N (2018) Intramolecular HB interactions evidenced in dibenzoyl oxalamide derivatives: NMR, QTAIM, and NCI studies. J Phys Chem A 122:199-208.

Dolomanov OV, Bourhis LJ, Gildea RJ, Howard JAK, Puschmann H (2009) OLEX2: a complete structure solution, refinement and analysis program. J Appl Crystallogr 42:339-341.

Frisch MJ, Trucks GW, Schlegel HB, Scuseria GE, Robb MA, Cheeseman JR, Scalmani G, Barone V, Petersson GA, Nakatsuji H, Li X, Caricato M, Marenich AV, Bloino J, Janesko BG, Gomperts R, Mennucci B, Hratchian HP, Ortiz JV, Izmaylov AF, Sonnenberg JL, Williams-Young D, Ding F, Lipparini F, Egidi F, Goings J, Peng B, Petrone A, Henderson T, Ranasinghe D, Zakrzewski VG, Gao J, Rega N, Zheng G, Liang W, Hada M, Ehara M, Toyota K, Fukuda R, Hasegawa J, Ishida M, Nakajima T, Honda Y, Kitao O, Nakai H, Vreven T, Throssell K, Montgomery JA Jr, Peralta JE, Ogliaro F, Bearpark MJ, Heyd JJ, Brothers EN, Kudin KN, Staroverov VN, Keith TA, Kobayashi R, Normand J, Raghavachari K, Rendell AP, Burant JC, Iyengar SS, Tomasi J, Cossi M, Millam JM, Klene M, Adamo C, Cammi R, Ochterski JW, Martin RL, Morokuma K, Farkas O, Foresman JB, Fox DJ (2016) Gaussian 16, Revision C.01. Gaussian Inc, Wallingford CT, USA.

Fukui K, Yonezawa T, Shingu H (1952) A molecular orbital theory of reactivity in aromatic hydrocarbons. J Chem Phys 20:722-725.

Garg U, Agrawal I, Azim Y (2025) Investigating crystal structure, chemical reactivity, and non-covalent interactions in the 1-naphthalene acetic acid -urea cocrystal by systematic computational methods. J Mol Struct 1325:140986.

Glendening ED, Badenhoop JK, Reed AE, Carpenter JE, Bohmann JA, Morales CM, Weinhold AJ, Weinhold F (2018) NBO 7.0, Theoretical Chemistry Institute, University of Wisconsin, Madison.

Grimme S, Antony J, Ehrlich S, Krieg H (2010) A consistent and accurate ab initio parametrization of density functional dispersion correction (DFT-D) for the 94 elements H-Pu. J Chem Phys 132:154104.

Heldt WZ (1958) Beckmann rearrangement. I. SYNTHESES of oxime p-toluenesulfonates and Beckmann rearrangement in acetic acid, methyl alcohol and chloroform. J Am Chem Soc 80:5880-5885.

Heller ST, Duncan AP, Moy CL, Kirk SR (2020) The value of failure: a student-driven course-based research experience in an undergraduate organic chemistry lab inspired by an unexpected result. J Chem Educ 97:3609-3616.

Hoffmann M, Rychlewska U, Warżajtis B (2005) The role of multiple parallel and antiparallel local dipoles for molecular structure and intermolecular interactions of oxalamides. CrystEngComm 7:260-265.

Jad YE, de la Torre BG, Govender T, Kruger HG, El-Faham A, Albericio F (2016) Oxyma-t, expanding the arsenal of coupling reagents. Tetrahedron Lett 57:3523-3525.

Jelsch C, Ejsmont K, Huder L (2014) The enrichment ratio of atomic contacts in crystals, an indicator derived from the Hirshfeld surface analysis. IUCrJ 1:119-128.

Johnson ER, Keinan S, Mori-Sánchez P, Contreras-García J, Cohen AJ, Yang W (2010) Revealing noncovalent interactions. J Am Chem Soc 132:6498-6506.

Keith TA (2013) AIMAll (Version 13.05.06), TK Gristmill Software, Overland Park, KS, USA.

Kelley SP, Smetana V, Nuss JS, Dixon DA, Vasiliu M, Mudring AV, Rogers RD (2020) Dehydration of $UO_2Cl_2{\cdot}3H_2O$ and $Nd(NO_3)_3{\cdot}6H_2O$ with a soft donor ligand and comparison of their interactions through X-ray diffraction and theoretical investigation. Inorg Chem 59:2861-2869.

Kolb HC, Finn MG, Sharpless KB (2001) Click chemistry: diverse chemical function from a few good reactions. Angew Chem Int Ed 40:2004-2024.

Lu T, Chen F (2012) Multiwfn: a multifunctional wavefunction analyzer. J Comput Chem 33:580-592.

Mackenzie CF, Spackman PR, Jayatilaka D, Spackman MA (2017) Crystalexplorer model energies and energy frameworks: extension to metal coordination compounds, organic salts, solvates and open-shell systems. IUCrJ 4:575.

Mahesha UKAH, Lokanath NK (2025) Structural and computational investigations of amide derivative: conformational, supramolecular analysis, and biological evaluation. J Mol Struct 1341:142604.

Molina-Paredes AA, Lara-Cerón JA, Ibarra-Rodríguez M, del Angel-Mosqueda C, Dias HVR, Jiménez-Pérez VM, Muñoz-Flores BM (2022) Supramolecular interactions in X-ray structures of oxalamides: green synthesis and characterization. J Mol Struct 1263:133144.

Morales-Santana M, Chong-Canto S, Santiago-Quintana JM, Martínez-Martínez FJ, García-Báez EV, Cruz A, Rojas-Lima S, Padilla-Martínez II (2022) Microcrystalline solid–solid transformations of conformationally-responsive solvates, desolvates and a salt of N,N′-(1,4-phenylene)dioxalamic acid:the energetics of hydrogen bonding and $n/\pi \rightarrow \pi^*$ interactions. CrystEngComm 24:1017-1034.

Orlandin A, Guryanov I, Ferrazzano L, Biondi B, Biscaglia F, Storti C, Rancan M, Formaggio F, Ricci A, Cabri W (2022) Carbodiimide-mediated Beckmann rearrangement of Oxyma-B as a side reaction in peptide synthesis. Molecules 27:4235.

Paul G, Bisio C, Braschi I, Cossi M, Gatti G, Gianotti E, Marchese L (2018) Combined solid-state NMR, FT-IR and computational studies on layered and porous materials. Chem Soc Rev 47:5684.

Podda E, Dodd E, Arca M, Aragoni MC, Lippolis V, Coles SJ, Pintus A (2024) N,N′-Dipropyloxamide. Molbank M1753.

Robello M, Barresi E, Baglini E, Salerno S, Taliani S, Settimo FD (2021) The alpha keto amide moiety as a privileged motif in medicinal chemistry: current insights and emerging opportunities. J Med Chem 64:3508-3545.

Sheldrick GM (2015) Crystal structure refinement with SHELXL. Acta Crystallogr C Struct Chem 71:3-8.

Spackman MA, Jayatilaka D (2009) Hirshfeld surface analysis. CrystEngComm 11:19-32.

Spackman MA, McKinnon JJ (2002) Fingerprinting intermolecular interactions in molecular crystals. CrystEngComm 4:378-392.

Spek AL (2003) Single-crystal structure validation with the program PLATON. J Appl Crystallogr 36:7-11.

Weigend F (2006) Accurate coulomb-fitting basis sets for H to Rn. Phys Chem Chem Phys 8:1057-1065.